Speed Variation Based Power Regulation Concept for Dynamic Wireless Charging

Donovin D. Lewis, *Student Member, IEEE*, Sudarshan T. Harave, *Member, IEEE*, Omer Onar, *Senior Member, IEEE*, Mostak Mohammad, *Senior Member, IEEE*, Veda P. Galigekere, *Senior Member, IEEE*, Gui-Jia Su, *Senior Member, IEEE*, and Dan M. Ionel, *Fellow, IEEE*

***Abstract*—On-road wireless charging of electric vehicles (EVs) in-motion could potentially reduce range anxiety or battery size with wide-spread deployment. The planning and implementation of such systems are greatly complicated due to their susceptibility to load variation inherent to traffic flow. This paper proposes a method for derisking the potential for traffic slowdowns by compensating for reduced vehicle speed and investigates how implementation may affect system performance. A load modeling case study is presented at 200kW for a mile of high-speed roadway employing speed-based power regulation with results indicating average power usage and maximum car hosting capability can be reduced by 20% and increased by 30% respectively. An 85kHz power electronics model is developed based on designs and prototypes for an 11kW, 190m airgap static system and a 200kW dynamic wireless track. The simulation is validated in the 11kW experimental prototype and modified for 200kW operation to compare with simulated performance. Sensitivity studies are performed in MATLAB/Simulink to evaluate how parameters influence system performance and confirm the capability to reduce output power and maintain efficiency at 11 and 200kW. The static 11kW experimental system operates at 93.6% efficiency and multiple options exist to reduce power while maintaining efficiency greater than 90%. The capability to dynamically modify power output from WPT coils, in an experimentally validated simulation, enables techniques to significantly mitigate load variability due to reductions in vehicle speed.**

***Index Terms*—Dynamic wireless power transfer (DWPT), electric vehicle (EV), wireless charging, sensitivity analysis, traffic flow.**

I. Introduction

The application of wireless power transfer (WPT) to charge electric vehicles (EVs) while they are driving has been proposed as a potential solution to alleviate range anxiety caused in part by limited infrastructure and long charging duration [1]. The introduction of dynamic wireless charging systems (DWCS) to roadways adds significant complexity to the sizing and system operation due to traffic-based variability and the implications of numerous edge case scenarios as suggested in [2]. Studies have found that electrification of 5-10% of primary roadways in the US with DWCS can cover almost all expected light duty vehicle drive cycles in charge-sustaining operation or allow for significant reductions in on-board vehicle battery size [3], [4]. Evaluation and mitigation of behavior inherent to roadway traffic can pave the way for full-scale deployment by derisking potential hazards and challenges.

Dynamic wireless charging uses electromagnetically coupled coil pairs to transfer near constant power from grid-connected, ground-embedded transmitters connected as a track under a traffic lane to receivers embedded in moving vehicles like the example shown in Fig. 1. Spacing and coil size can be adjusted to facilitate uniform power transfer in the receiving coil regardless of rated power like that discussed in [5] and [6] but system-level power demand depends on traffic behavior. As such, there would exist high minute to minute variability in location-specific power demand which may cause a disturbance in power grid stability like mentioned previously in [7]. DWCS development benefits from the interdisciplinary integration of component-level power electronics control with systems-level traffic-based load modeling.

Integrated control of component-level power electronics depending on response at the systems-level traffic behavior enables the potential mitigation of susceptibility to vehicle count and speed variation. Optimal design of coil size, spacing, and converter segmentation was proposed in [8] considering necessary distance between cars and maximum speed. Methods of segmentation and lane diversion were further developed in [9] to compensate for a large load expected during peak periods with integrated battery energy storage. A method was proposed in [10] to reduce load on a target roadway significantly by selectively charging vehicles which are below a defined maximum state-of-charge. Operational modification with speed was proposed in [11] by modifying vehicle-side resistance to reduce power fluctuation with varying speeds and achieve charge-sustaining operation.

The impact of vehicle speed on efficiency of transferred energy was studied in [12] with suggestions to limit speeds within an allowable band for enhanced charging performance. Output power may be controlled by grid-side power electronics depending on the speed and number of vehicles as suggested in [13]. The modification of power delivered to vehicles depending on speed was also explored in [14] to increase energy transferred, enabling charge-sustaining mode at higher speeds. Previous studies pairing traffic modeling and energy transfer have indicated that the energy transferred to each car and impact on the grid can vary significantly on vehicle speed but have not analyzed the impacts of traffic speed reduction on high-speed roadways during peak periods [15]–[17].

Implementations of dynamic wireless charging in laboratory settings are either very limited in track length, allowing for the

equivalent of one car at a time, or at very small scale such as the example implementations in [18]–[22]. While a few full-size experimental tracks exist worldwide, such as, for example, from startups such as Electreon [23], CIRCE [24], and ENRX [25], they are proof-of-concept implementations that are limited to 20kW and small-scale relative to the expected speed of travel, yet require multi-million-dollar investment. Once the system is deployed on the road it cannot be derisked due to the massive investment and commitment required for full-scale deployments. The simulations in this paper, benefiting from experimental prototype results, are introduced as a method to derisk multiple aspects of future implementation without the very large investment typically required.

In currently planned DWCS, vehicles will receive the same power at all speeds, resulting in more energy transferred at lower speeds due to more time on the track. If power is maintained at all speed conditions, DWPT equipment would have to be significantly oversized for congested traffic conditions and may be cost prohibitive for deployment. The development of down regulating power based on speed derisks multiple aspects including energy delivered to vehicles during traffic slowdowns and potential slowdowns caused by cars decelerating for increased charge. The proposed concept scales transmitted power linearly with reduced speed to deliver a predefined maximum energy to each vehicle with the secondary effect of maximizing the number of cars that can be charged simultaneously on the roadway.

This paper presents a method of mitigating potential challenges due to driver speed behavior and derisk dynamic wireless charging system (DWCS) implementation with systematic control of output power. The major contributions include a method of dynamic wireless charging load compensation for reduced vehicle speed, a model for traffic modeling of high-speed roadways at second resolution, and power electronics simulation/experimentation to verify the capability to reduce power and maintain sufficient efficiency. A model for DWCS load analysis was developed and implemented at second resolution, including comparison between minute and second-based modeling for a high-speed interstate. Power electronics models and prototypes, developed in MATLAB/Simulink and experimentally validated, were used to study system performance with reduced power output and varying speeds.

This paper is a follow-up expansion of two previous conference papers by the same group of authors [26], [27]. New contributions relative to the conference papers include further development of the resolution comparison for traffic simulation on high-speed roadways, unified T-model power electronic simulations for 11kW and 200kW systems, and a full design of experiments for optimal reduction of power output with minimal impact on efficiency.

Section II describes a method for dynamic wireless charging traffic simulation with reasoning for sub-minutely resolution on high-speed roadways. Section III proposes a method of controlling output power to maximize electric vehicle hosting capability on a wireless charging roadway. Section IV introduces the power electronics simulation used to evaluate the impact of modifying key control parameters and reduce output power per coil. Section V describes the static 11kW and dynamic 200kW experimental studies which validated the simulation results and parameter selection to maximize efficiency at reduced power. A detailed simulation discussion and case study is described in Section VI at 200kW rated power employing the proposed power sharing method and control parameter variation. Section VII includes a discussion of high power specific implementation including a simulation varying coupling coefficient and evaluating efficiency.

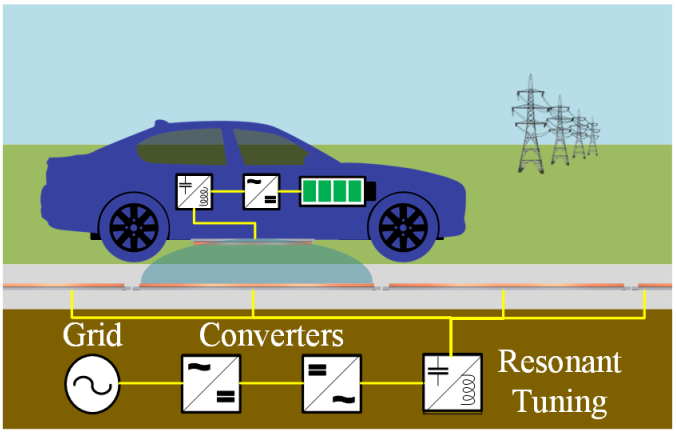

Fig. 1. A diagram of an example wireless power transfer system for charging electric vehicles with power-systems level control and power electronics control to compensate for variability.

II. Traffic-based DWCS Load Simulation

Load profiles and grid impact of DWCS systems are highly dependent on the location-specific behavior of vehicles on the roadway. Ideally, sub-minutely sensing data such as GPS-stamped driving cycles or weigh-in-motion data would be collected and available prior to larger system planning such as in [28] and [29] respectively. Due to the lack of widespread publicly available high-resolution traffic data, several models have been proposed to simulate roadway traffic and resulting power by stochastically interpolating vehicle time of arrival and assuming constant vehicle speed from data at, for example, one-hour resolution to lower resolutions to the minute time step as in [30], [31] or second resolution in [32], [33]. The resulting synthetically generated DWCS load can aid in system planning by predicting average and peak demand.

To approximate the expected load on a target roadway, a traffic model for synthetic data generation was improved upon from [9] with second time resolution and the proposed speed based power regulation concept. Interpolation of sub-hourly vehicle arrival and vehicle speed sampling is described in the following equations and distributions:

$$V_a(h) = \frac{N_h(h)}{\sum_{h=0}^{23} N_h} * AADT = P(h) * AADT, \quad (1)$$

$$V_a(n) = \frac{e^{-\lambda * t} * (\lambda * t)^n}{n!} \text{ where } \lambda = V_a(h) * \Delta(t), \quad (2)$$

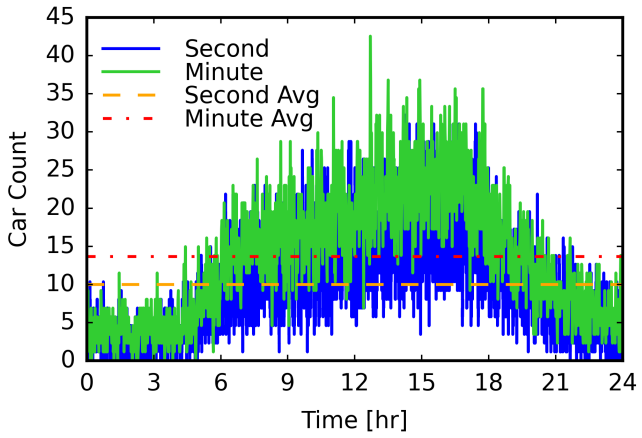

Fig. 2. Example number of cars on the Bowling Green, KY interstate with varying simulation time resolution at 70mph average speed ±15mph.

$$S_v(V) = \frac{1}{\sigma\sqrt{2\pi}} * e^{-\frac{1}{2}(\frac{V-\lambda}{\sigma})^2}, \tag{3}$$

where $V_a(h)$ is the number of vehicles per hour on the roadway; $AADT$, the recorded annual average daily traffic; $P(h)$, the percentage of cars per day to arrive on the road per hour; $V_a(n)$, the number of vehicles arriving at every timestep; λ, either the hourly vehicle count or speed limit; Δt, the time resolution in seconds; σ the standard deviation of speed; and $S_v(V)$, the speed sampled for of individual vehicles.

Equation (1) estimates the number of vehicles per hour on the roadway as a product of the annual average daily traffic (AADT) and the percentage of cars per day expected to arrive on the road at that hour. A Poisson distribution, represented by (2), is used to approximate the number of vehicles arriving at every second using the hourly vehicle count as the mean. For each vehicle, a normal distribution with the speed limit as the mean is sampled per vehicle for a constant speed while on the roadway in (3). Combining all three equations, the number of vehicles arriving at a time step is sampled from (2) using a mean calculated relative to the AADT in (1) and each vehicle's speed is sampled from (3). The time left on the roadway is decreased per time step in proportion to the vehicle's constant speed until the vehicle exits the section of road. The number of vehicles on the roadway is counted at each time step and multiplied with the wireless charging coils rated power to estimate the aggregate load considering one vehicle is coupled to one coil or coil pair at any time step.

Sub-hourly traffic data was estimated using AADT provided from the Kentucky Transportation Cabinet's Interactive Statewide Traffic Counts Map [34] and an hourly traffic distribution (HTD) from 900+ days of hourly Automated Traffic Recorder (ATR) traffic counts. The studied highway is one mile of highway interstate I-75 near Bowling Green, KY which has a maximum speed limit of 75mph. A minimum speed limit of 55mph is assumed following typical traffic laws restricting speed to within 15mph below the speed limit. A transmitter coil length of 1.73 meters is assumed with only one car activating a single coil at any point in time. All cars are assumed to be electrified and WPT capable with the potential to charge multiple vehicles at the same time.

Unlike conventional traffic modeling where minute resolution is sufficient, the length of the studied roadway and average vehicle speed can necessitate sub-minutely time resolution to estimate expected variability. For example, a one-mile roadway with speeds greater than 60mph requires simulation at a sub-minutely timestep to accurately approximate average and maximum power demand. If the average vehicle speed is 70mph and the roadway is 1 mile long, then the average crossing is 51 seconds and minutely models would only see a peak at the beginning of the minute with very little overlap between minute periods. As a result, minute-based vehicle arrival estimation overestimates maximum power expected due to peaks at each minute and underestimates average power as it does not fully represent the duration of travel across the roadway.

Example car counts varying in time with second and minute resolution are shown in Fig. 2. An average load curve was calculated from 10 synthetically generated loads at second and minute resolutions. The maximum instantaneous power and average power is 21% and 16% higher respectively with minute resolution compared to second resolution. For the studied roadway length and average speed, the minute-based vehicle arrival approximation leads to a peak of cars at the minute transition, artificially increasing maximum and average power as expected. Simulation at a second time step distributes when cars enter the roadway, ensuring that increased power due to overlap in vehicles is also taken into account.

III. Power Regulation Concept Based on Speed

Power demand in DWCS varies greatly depending on the speed of traffic and energy transferred to vehicles accordingly can be approximated as:

$$E(V) = P * \eta * \left(\frac{L_t}{S_v(V)}\right), \tag{4}$$

where η is the efficiency, L_t the length of the track, and $S_v(V)$ the speed of the vehicle. Reductions in vehicle speed at a constant rated power increases the energy transferred to individual cars but reduces the maximum number of cars that can be charged simultaneously. The impact of reduced speed on the maximum number of concurrent cars can be approximated as a product of the maximum concurrent cars at the base speed and the ratio between the defined minimum and base speed. Ensuring a maximal number of cars can be charged concurrently enables the opportunities for charge-sustaining operation or reduction in on-board battery size.

Localized dynamic power electronics control like the example in Fig. 3 can alter system parameters depending on vehicle speed. Three variables are considered for alteration of power electronic control to reduce output power: V_{dc}, input DC voltage; f_s, switching frequency for the inverter; and d, the duty cycle for phase shift inverter control. The command power varying with speed, P_s, is controlled with the proportional

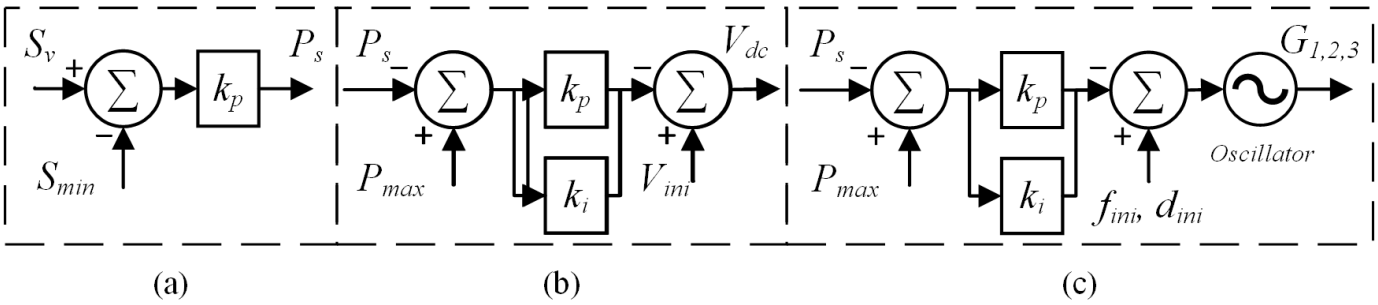

Fig. 3. Proposed controls to adjust power output using (a) the difference between the minimum defined speed and vehicle speed with (b) variation in DC bus voltage and (c) modification of inverter frequency and duty cycle.

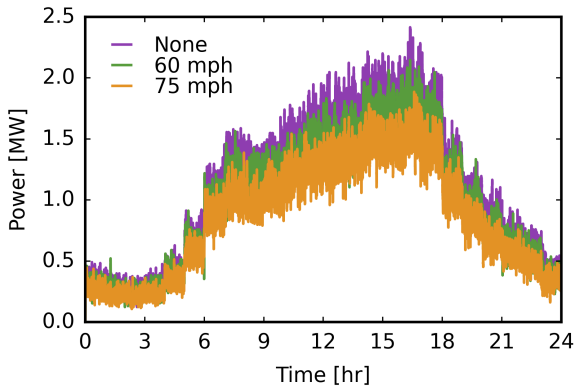

Fig. 4. Power profiles for the Bowling Green, KY interstate case varying the minimum speed for power sharing with 25% vehicle electrification.

controller example in Fig. 3(a). By reducing power delivered to vehicles traveling slower than the defined minimum speed, traffic slowdowns can be prevented from drivers desiring increased charge, more vehicles can be charged simultaneously for a fixed maximum loading, and primary side equipment doesn't have to be oversized such that cost can be minimized.

Speed proportional reduction of rectified DC voltage supplied to the inverter reduces output current for a set load, allowing for direct control of power as depicted in Fig. 3(b), similar to that performed in [35]. The modification of controls for DC voltage would ideally be applied to active power factor correction (PFC), such as those in [15], [36]. The capability for DC bus voltage control using the PFC is limited but an additional buck converter can be added after the rectifier to down regulate DC bus voltage directly. Switching frequency and duty cycle of the inverter can be modified by using the output of similar PI controllers to vary the oscillator used for switch gating signals like depicted in Fig. 3(c).

Selection of the minimum speed depends on the average speed, standard deviation of speed, length of the roadway, and maximum WPT coil power. Traffic behavior was synthetically generated using the improved traffic model with speed based power regulation for minimum speeds in 1 mph intervals from 55 to 75mph, average speed of 65mph, and speed standard deviation of $\pm$ 15mph. This process was repeated 30 times per minimum speed and averaged to isolate random variation due to the speed variation. Resulting load profiles are depicted in Fig. 4 for three example minimum speeds. The resulting average power and maximum power expected for the averaged loads per minimum speed was compared with an average load without speed based power regulation using the same speed average and standard deviation.

The implementation of speed based power regulation in this study resulted in average and maximum power reductions up to 21% and 24% respectively for the roadway. A 1-dimensional least squares polynomial fit between average load reduction and minimum speed resulted in the following equation: $P_{avg} = 0.71S_v - 33.4$, where P_{avg} is the percentage in average power reduction and S_v is minimum speed in miles per hour. Studies similar to this one can enable the systematic definition of minimum speed for the roadway based on the trade-off between speed and power flexibility for consumers and mitigation of large load variability.

IV. Power Electronics Simulation

A power electronics simulation was developed in MATLAB/Simulink for a unidirectional LCC-S compensated wireless power transfer to explore methods of modifying power delivered to individual cars in response to reduced speeds while maintaining high efficiency. A diagram of the model is shown in Fig. 5 with scope extending from the AC grid rectified and power factor corrected DC supply bus to the resistive load of the EV battery pack. Grid-side rectifying and power factor correction (PFC), like those reviewed in [37] would also be necessary but operational effectiveness of this portion could vary significantly depending on the localized grid strength and accordingly selected topology. As a capacitor is typically used in the DC link to operate as a voltage source, this can be represented as a DC source for simulation and experimentation. With the latest silicon carbide wide band gap technology, power losses are expected to be low throughout the entire operation range with frequency and load.

The DD coil used for the study is around 6ft wide correlating with average vehicle width on a 12ft wide road so there is a chance for misalignment. However, advanced technology perfectly center the vehicle in the lane, such as active line tracking or line centering driver assist systems, are increasingly common in new vehicles. While there may be slight reductions in efficiency and power with misalignment

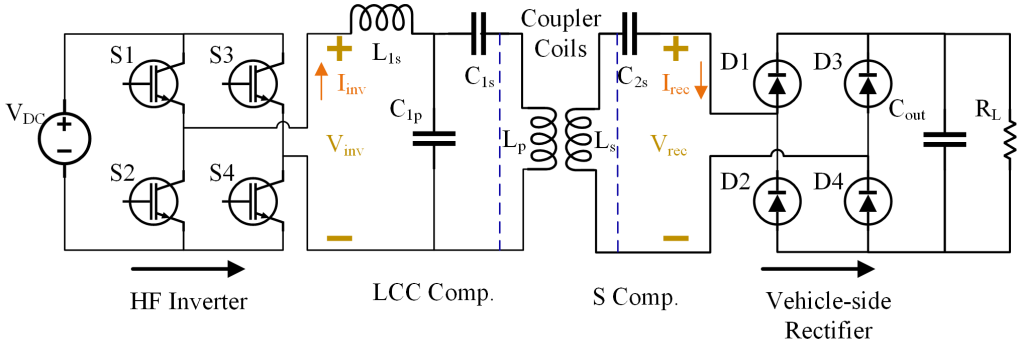

Fig. 5. Schematic of the LCC-S WPT power electronics simulated and experimentally evaluated to study the sensitivity of system performance to alteration of control parameters for traffic speed based power regulation.

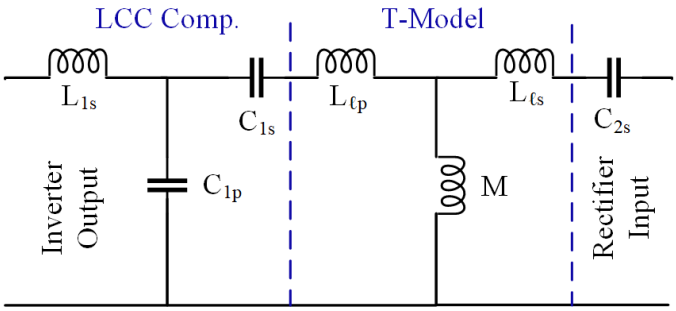

Fig. 6. T-model circuit used for 11kW and 200kW simulation with a constant or time-varying coupling coefficient considering the overlap between vehicle-side and ground-embedded coils.

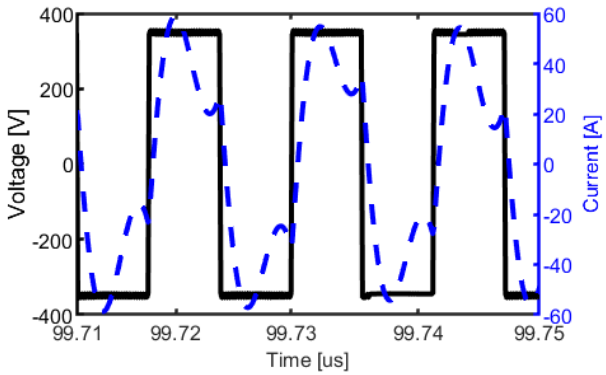

Fig. 7. Example simulated voltage and current output waveforms from the 11kW 85kHz inverter with ZVS operation.

due to the large increase in lane centering technology, lateral misalignments aren't as much of an interest.

Primary-side compensation consists of an LCC circuit allowing for continuous output current and control depending on a tuning inductor value that can change coil current from the primary. Unidirectional power transfer allows for secondary-side series capacitor compensation without the concern for complex output tuning. The LCC-S resonant tuning bank was used to minimize the size and complexity of onboard secondary compensation and reduce transmitter power in the absence of cars on the roadway. Compensation circuit parameters were calculated based on the simplified process described in [38] with output power greatly controlled by the size of the primary inductance:

$$L_{1s} = M\frac{V_{in}}{V_{out}}, \tag{5}$$

$$C_{1p} = \frac{1}{\omega^2 L_{1s}}, C_{1s} = \frac{1}{\omega^2}\frac{1}{L_p - L_{1s}}, C_{2s} = \frac{1}{\omega^2 L_s}, \tag{6}$$

where, L_{1s} is the primary series inductor value; $M = k\sqrt{L_p * L_s}$ the peak mutual inductance; V_{DC} and V_{out} are the AC voltage input and voltage output respectively; C_{1p} is the parallel capacitor value for the primary; C_{1s} the primary series capacitor value; ω the angular frequency; L_p the transmitter inductance; C_{2s} the secondary series capacitance; and L_s the secondary inductance.

A T-model representation, from [35] and depicted in Fig. 6, was used for the primary and secondary transmitter coils to allow for simulations with a varying mutual inductance correlated with changing relative position and speed. The equations for the respective components are as follows:

$$M = k * \sqrt{L_p * L_s}, L_{lp} = L_p - M, L_{ls} = L_s - M, \tag{7}$$

where M is the mutual inductance, k the coupling coefficient, L_p and L_s the self-inductances of the primary and secondary respectively, and L_{lp} and L_{ls} the leakage inductances of the primary and secondary.

Device-level parameters were directly adapted from previous experimentation, for example, on-state resistances, near 4mΩ, and diode forward voltages of 2V from [39]. Output DC link capacitors were specified as 100μF to mitigate current ripple related to high frequency switching. In the 11kW model, primary and secondary coupler coil self-inductances of 53 and 44.5 μH were derived from an experimental prototype developed in [40]. Primary and secondary self-inductances of 7.4 and 22.47 μH for 200kW operation were adopted from a previous validated simulation in [41]. Various additional parameters for the simulation and experimental studies are detailed in Table I where Rds_{on} is inverter on-state resistance and R_{misc} is the assumed resistance for passive elements.

A maximum coupling coefficient of 0.15 was assumed for both rated powers as a typical value for a large airgap as

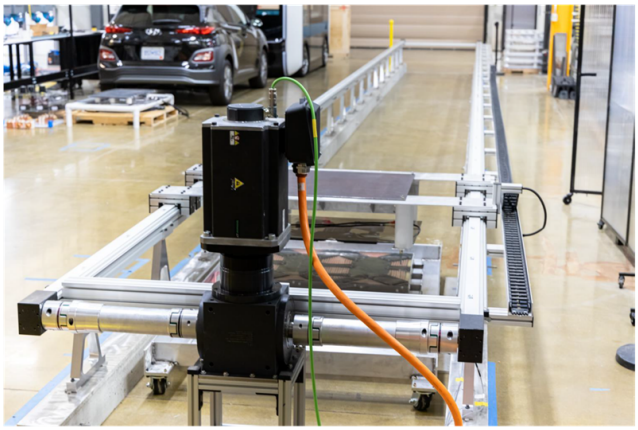

Fig. 8. Dynamic wireless charging track using a moving platform for the vehicle coil capable of 20mph speed and a stationary transmitter coil.

reported in a number of prior studies [1], [41], [42]. As dynamic wireless EV charging is still in the very early days of development, the question of whether to space coils tightly or space them out is still of debate by various groups with potential issues including regulation of power and coupling to the body of the car. Studies considering varying coil spacing and position-varying coupling coefficient are described in Section VI and Section V respectively. To study the impacts of known power electronic system quantities on performance with varying command powers, an ideal coupling coefficient is considered for the parametric studies assuming tightest possible coils for the application and with the understanding that variation in spacing can significantly impact efficiency.

V. Experimental Testing and Results

A combination of results for 85kHz static and dynamic wireless charging experimental prototypes were used to study expected performance variation with movement across the track and systematic reduction in power output respectively. Due to the cost-intensive nature of at-scale prototyping of dynamic wireless charging test setups, previous studies, such as in [13], [43]–[45], have used a mixture of small-scale static wireless charging prototypes with assumptions based on dynamic operation. These methods allowed for development and testing of new controls and designs for dynamic wireless charging in laboratory settings without very costly full deployments.

Within this study, results from a dynamic wireless charging track, shown in Fig. 8 and detailed in [46], was used for a study of coil spacing to characterize potential performance variation with at-scale movement. The 18 meter track was used for dynamic mode validation using a moving platform with the vehicle-side coil and power electronics and a stationary transmitter coil, of the same sizes as used in the traffic modeling. The profile of measured output power and efficiency for the 200kW dynamic charging system was captured while mimicking vehicle motion along the track by measuring along the length of the transmitter at discrete points.

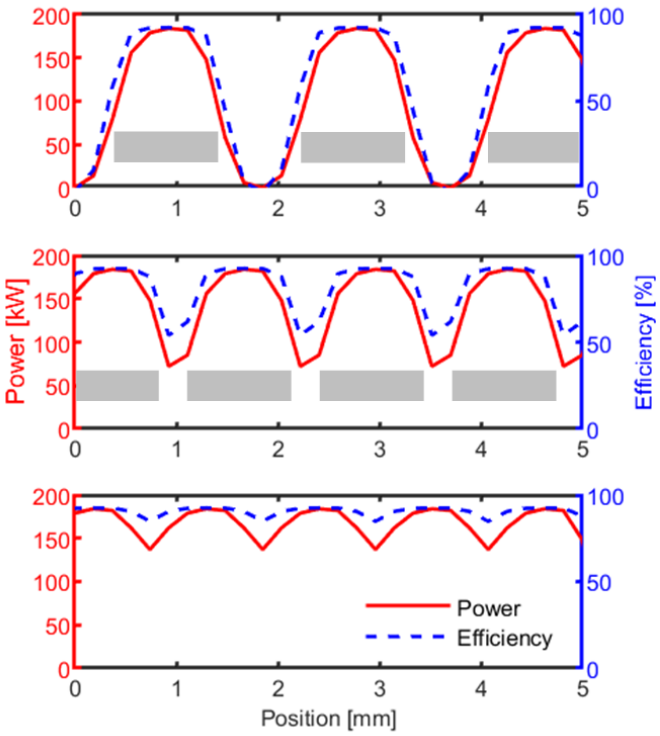

Fig. 9. Experimentally based study of coil spacing using laboratory track measurements. The light gray blocks represent example transmitter coils.

The experimental results for power and efficiency from [47] were then used for an analytical study varying coil spacing, shown in Fig. 9, using a polynomial fit of the power to efficiency measured with coil power profiles at varying coil gaps. Estimation in this way may underestimate efficiency as it assumes the passive components have no storage between coil charges but it allows observations without deploying multiple coils directly. The results suggests that performance can vary greatly depending on coil spacing with dips in efficiency for cases such as in the top plot when one coil is activated at a time. Alternatively, an ideal continuous track with tightest possible spacing could allow for near constant coupling using adjacent coils with alternating winding directions to ensure positive coupling without field cancellation.

The 11kW static wireless charging prototype, first described in detail in [48], was then used to study expected performance variation with a systematic reduction in power output using the assumptions from the dynamic study. A picture of the static experimental setup is shown in Fig. 10 with annotations denoting system components including a DC load operating as a battery emulator, the coupling coils, primary side inverter, and the tuning network. The high frequency inverter , operating at 85kHz to comply with SAE J2954 recommend practice, uses 1200V/325A Wolfspeed/CREE CAS325M12HM2 SiC MOSFET phase-leg power modules in an H-bridge configuration with CGD15HB62LP gate drivers. The rectifier on the vehicle-side uses 600V/100A APT2X101DQ60J phase-leg rectifier modules in a dual die isotope package. The prototype coil pair

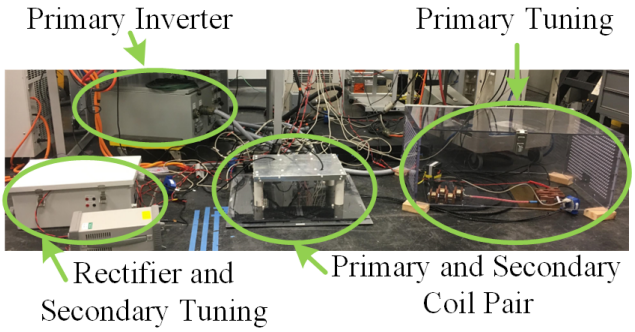

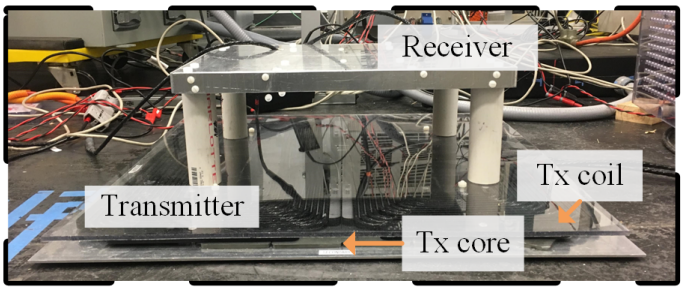

Fig. 10. Experimental 11kW, 85kHz stationary wireless EV charging test system (a) and a detailed view of the DD coil prototype (b).

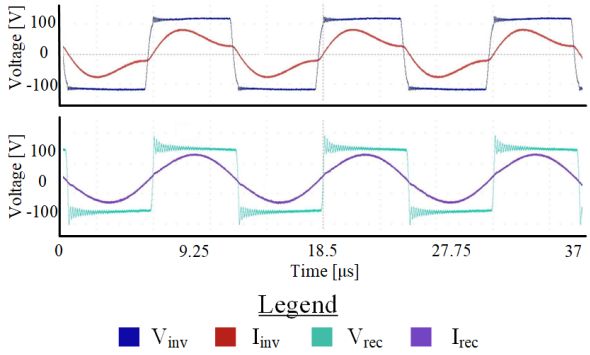

Fig. 11. Voltage and current waveforms measured at the inverter and rectifier in the 11kW stationary wireless charging prototype.

consists of 6AWG Litz wire of four primary turns and eight secondary turns with Ferroxcube 3C95 ferrite tiles of 5mm thickness for an overall area of 711x711mm and 381x482mm in the primary and secondary respectively.

The static 11kW prototype was tested at the parameters specified in Table I. The resulting performance was measured at various stages using a power analyzer, with results shown in Fig. 12. The efficiency of the inverter, η_1; resonant tank and coils, η_2; and rectifier, η_3; were 99.7%, 94.8%, and 99.0% respectively for a combined DC-DC efficiency, η_4, of 93.6%. Due to the additional internal resistances, wire lengths, interconnects, and non-ideal properties and component parasitics, the experimental efficiency may be slightly less than what is estimated in simulations. The measured operational waveforms of the voltage and current output from the inverter, V_{inv} and I_{inv}, and voltage and current input to the rectifier, V_{rec} and I_{rec}, are shown in Fig. 11. The inverter output waveforms matched with the simulated results shown in Fig. 7 and the rectifier input indicates effective secondary-side series compensation.

VI. Sensitivity Analysis Results

Two models were developed, one at 11kW to enable small-scale experimentation and simulation validation and another at 200kW, using the same modeling logic and principles. Within

TABLE I
Experimental and Simulation Parameters for the 11kW, 190mm Airgap, 85kHz Stationary Wireless Charging System.

Parameter	Experimental Value	Simulated Value
L_{1s}	15μH	12μH
C_{1p}	200nF	292nF
C_{1s}	55nF	56nF
C_{2s}	41nF	41nF
Rds_{on}	2.29mΩ	3.7mΩ
R_{misc}	$> 1m\Omega$	1mΩ

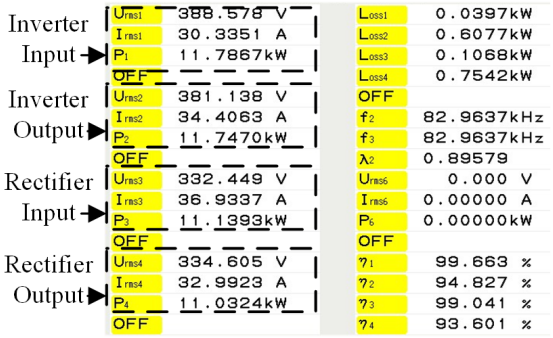

Fig. 12. Power analyzer measurements for the 11kW stationary wireless charging prototype at the inverter input, inverter output, rectifier input, and rectifier output.

each model, input power, output power, and maximum achievable DC-DC efficiency were calculated with a parametric sweep of the primary-side switching frequency, high-frequency duty cycle, and input DC voltage. Simulation results indicate a DC-DC efficiency of 93% at 85kHz, 11kW operation with 400V DC input and a duty cycle of 1 or 50% pulse width.

The development of models for 200kW were developed from the calibrated and experimentally validated 11kW system. Typical high power wireless charging systems also include an advanced system for voltage regulation with additional controllable switches on the vehicle-side. Those DC-DC converters were not included to allow for the direct comparison with the experimental 11kW system and the capability to regulate voltage dynamically has been thoroughly covered in previous studies. The DC voltage input was adjusted to 800V and self-inductances were modified for 200kW operation. The

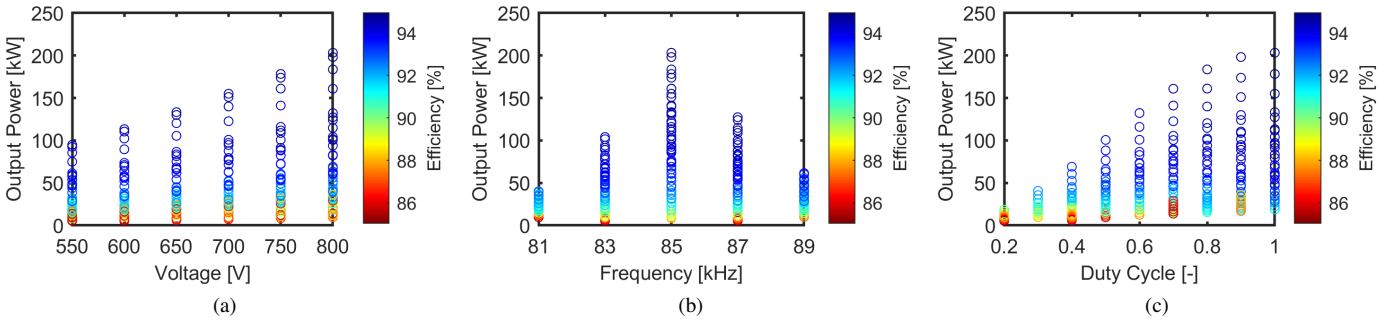

Fig. 13. Simulation results for a full design of experiments at 200kW steady-state operation varying: (a) input DC voltage, (b) switching frequency, and (c) inverter duty cycle.

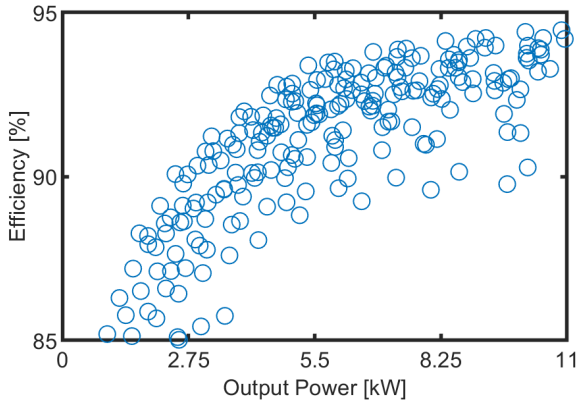

Fig. 14. Simulated steady-state efficiency results following parametric studies for various operating points in an 11kW rated system.

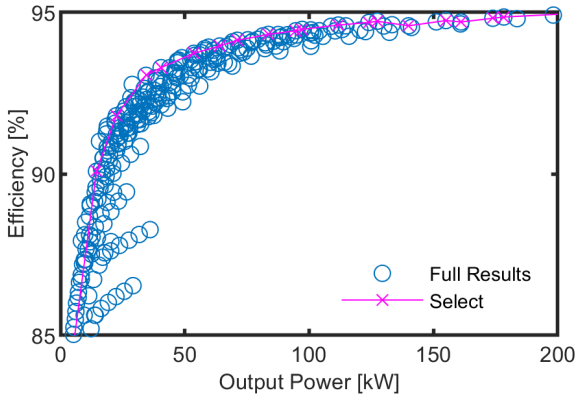

Fig. 15. Simulated steady-state efficiency results following parametric studies for various operating points in a 200kW rated system.

resulting model has a DC-DC efficiency of 94% at 85kHz, 200kW steady-state operation with comparable performance to a similar system that has been experimentally validated to 93% efficiency at 188kW, 85kHz operation in [39].

Inverter output voltage and resulting power transferred to the load varies as a function of the duty cycle, switching frequency, and input voltage with the relationship:

$$V_{inv} = \frac{4V_{in}}{\pi} \sin\left(\frac{d\pi}{2}\right) \cos(\omega t), \tag{8}$$

where V_{inv} is the inverter output voltage, d is the duty cycle of the high-frequency inverter, and ω is the angular frequency of the waveform. To explore the relationship between the three variables herein, sensitivity analysis was performed assuming a black box for system behavior. The Sensitivity Analysis toolbox from MATLAB was employed to perform design of experiments between parameters and resulting efficiency. Within this toolbox, ranges for each parameter were selected and applied with requirements, to maximize efficiency and minimize distance to the command power.

A full factorial design of experiments was performed with the 200kW model varying three control parameters: duty cycle from 0.1 to 1 in increments of 0.1, input DC voltage from 550 to 800V in increments of 10V, and switching frequency from 79-91kHz with increments of 1kHz. Control inputs were manually picked to provide maximum efficiency for a target output power for the three control parameters. At low power, system efficiency dipped as low as 78% with independent parameter modification but the optimal combination of parameters found a best possible efficiency of 81% at light load conditions. The resulting selected parameter combinations are presented in Table II from 40 to 200kW in 20kW increments.

The full results for output power and efficiency considering individual parameter variation are depicted in Fig. 13 with input voltage (a), frequency (b), and high-frequency duty cycle (c) respectively. Modification of the voltage directly reduces the expected output power without largely sacrificing the overall efficiency until the limit of DC bus voltage reduction mentioned in Section III is reached. Utilization of the resonant 85kHz transmission frequency is essential for high 200kW power and maintain efficiency greater than 85%, with slight advantages at higher frequencies, as expected, compared to the lower end of range. Altering the phase-shift duty cycle greatly alters both power capability and efficiency with low values between 10-20% resulting in significantly lower power and efficiency. Based on these results, a proposed combination to fulfill the rated power while managing reduced efficiency would be to first reduce input DC bus voltage using the active PFC followed by reducing the phase-shift duty cycle and with a final option of reducing switching frequency.

A summary of efficiency and output power results for the steady-state studies at 11kW and 200kW are shown in Figures

TABLE II
SELECTED PARAMETERS FOR VARYING COMMAND POWERS AND THE RESULTING MAXIMUM EFFICIENCY IN A SIMULATED 200KW SYSTEM.

Command Power [kW]	V_{dc} [V]	f_s [kHz]	d [-]	η [%]	P_{out} [kW]	Speed [mph]
40	650	89	1.0	93.29	40	15.0
60	600	87	0.8	93.96	64	22.5
80	650	87	1.0	94.32	84	30.0
100	700	87	1.0	94.48	97	37.5
120	800	87	0.9	94.69	124	45.0
140	700	85	0.8	94.59	140	52.5
160	750	85	0.8	94.70	161	60.0
180	750	85	1.0	94.86	178	67.5
200	800	85	1.0	94.95	203	75.0

14 and 15 respectively. One notable difference between the two studies is that the 200kW steady-state efficiencies are much tighter to the most optimal solutions, as expected, as the high efficiency is very necessary to achieve the command power. From the 200kW results, the most efficient solutions within each command power band were selected and are indicated with the star and line between on Fig. 15. The operating parameters necessary to reach these maximum operating efficiencies, at the command power are gathered in Table II.

VII. Discussion on High Power Specific Implementation

Speed compensation was employed within the traffic simulator for 200kW rated power with a speed standard deviation of $\pm$15mph and a range of minimum speeds from 55 to 75mph. As the defined minimum speed was increased, average and maximum load was reduced as slower cars are charged with less power. The resulting energy transferred to each vehicle is much more predictable with the standard deviation of energy transferred reduced by half, enabling easier planning for charge-sustaining operation. Methods of traffic modeling with speed-based power regulation are generally applicable to other roadways assuming sufficient data availability.

Power electronic simulations at 200kW indicate a potential power reduction by more than 40% while maintaining efficiency greater than 90%. Assuming a maximum 15mph or 21% drop in speed for the example roadway, the modification of DC input voltage alone could allow for satisfactory power sharing operation. Depending on the fluctuation of speed on the target roadway, this reduction of output power could also extend system lifetime by reducing high power stress.

An additional 200kW case was created with a time-varying coupling coefficient to compare performance to the previous simulations with constant coupling. Within this scenario, power was reduced prior to vehicle arrival assuming sufficient speed measurements. Using the traffic simulation, a power profile was created which varies power output by modifying the DC input voltage relative to vehicle speeds of 80mph and 55mph. The resulting input and output power of the DC-DC system is shown in Fig. 16 alongside the time-varying coupling coefficient. The energy transferred at both speeds was calculated using trapezoidal integration to be 18.92 Watt-seconds. The efficiency, as expected, was sustained at 55mph

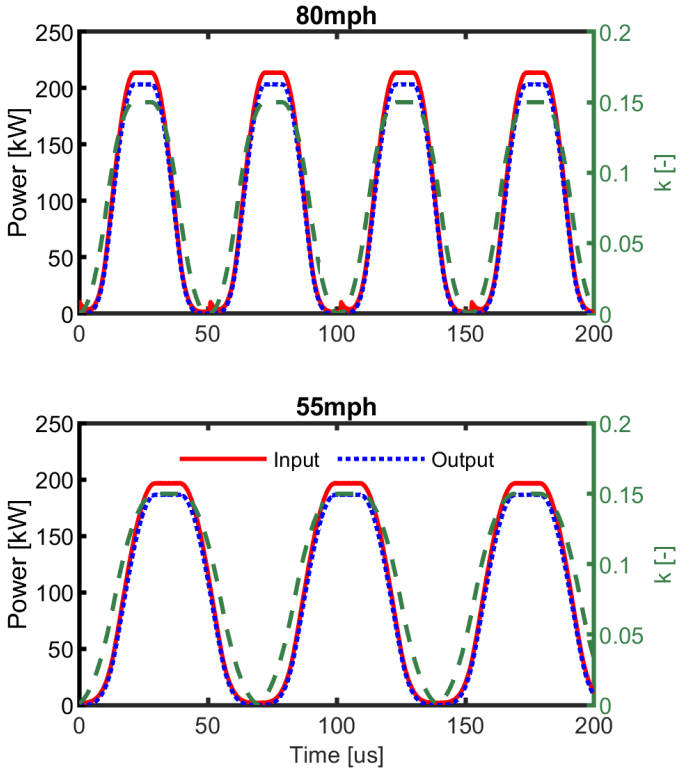

Fig. 16. Simulated case study of dynamically varying mutual inductance and input power with the resulting DC-DC output power. Efficiency is maintained sufficiently high throughout operation at the reduced power level.

operation with 7% reduced output power and peak efficiency of 93 to 94%.

The integration of power electronics and traffic modeling enables enhanced planning and operational control to accommodate the largest number of consumers possible. Advanced unified monitoring of the vehicle status, communication with centralized DWCS control, and the capability to alter power electronic controls accordingly is necessary to modify transmitted power as proposed. Rather than modification of the speed limit, localized control of the system depending on vehicle speed can mitigate system load, while managing energy transfer without system-wide or component-level changes.

VIII. Conclusion

A new method was proposed to regulate power based on the speed of vehicles in a dynamic wireless charging system to equalize energy transfer per vehicle. Implementation on high-speed roadways can derisk multiple aspects including potential oversizing of DWPT equipment to handle traffic congestion and increased traffic jams and slowdowns caused by drivers who want more charge. Second-resolution load modeling was developed for a high-speed interstate dynamic wireless charging system using localized measured automated traffic recorder data and sampled statistical distributions. Systems-level results found that compensating for speed reduction ($\leq$15mph) significantly reduced maximum instantaneous power demand by 24% and the average power by 21%.

Power electronic simulations developed in MATLAB/Simulink were validated with experimental results for a static 11kW system. Simulations were developed for 200kW rated power using assumptions and experimental results for a dynamic wireless charging track. Multiple methods were used to evaluate the capability to reduce power while maintaining sufficient performance with static steady-state and dynamically varying mutual inductance. The design of experiments and sensitivity studies found that output power can be reduced sufficiently, by more than 10%, at either power level without reducing the maximum achievable efficiency below 90%.

ACKNOWLEDGMENT

This work was supported by the National Science Foundation (NSF) Graduate Research Fellowship under Grant No. 2239063. This research used results from resources developed and available at the Power Electronics and Electric Machinery Research Facility located at the National Transportation Research Center, a U.S. Department of Energy (DOE) Efficiency and Renewable Energy User Facility operated by the Oak Ridge National Laboratory (ORNL), Knoxville, TN, USA. Any findings and conclusions expressed herein are those of the authors and do not necessarily reflect the views of the NSF or DOE. The support of the University of Kentucky, the L. Stanley Pigman Chair in Power endowment is also gratefully acknowledged.

REFERENCES

[1] S. Li and C. C. Mi, "Wireless power transfer for electric vehicle applications," *IEEE Journal of Emerging and Selected Topics in Power Electronics*, vol. 3, no. 1, pp. 4–17, 2015.

[2] A. Ahmad, M. S. Alam, and R. Chabaan, "A comprehensive review of wireless charging technologies for electric vehicles," *IEEE Transactions on Transportation Electrification*, vol. 4, no. 1, pp. 38–63, 2018.

[3] A. Foote, B. Ozpineci, M. Chinthavali, and J.-M. Li, "Sizing dynamic wireless charging for light-duty electric vehicles in roadway applications," in *2016 IEEE PELS Workshop on Emerging Technologies: Wireless Power Transfer (WoW)*, 2016, pp. 224–230.

[4] B. J. Limb, T. H. Bradley, B. Crabb, R. Zane, C. McGinty, and J. C. Quinn, "Economic and environmental feasibility, architecture optimization, and grid impact of dynamic charging of electric vehicles using wireless power transfer," in *6th Hybrid and Electric Vehicles Conference (HEVC 2016)*, 2016, pp. 1–6.

[5] A. Foote, O. C. Onar, S. Debnath, M. Chinthavali, B. Ozpineci, and D. E. Smith, "Optimal sizing of a dynamic wireless power transfer system for highway applications," in *2018 IEEE Transportation Electrification Conference and Expo (ITEC)*, 2018, pp. 1–6.

[6] T. M. Newbolt, P. Mandal, H. Wang, and R. Zane, "Diverse effects of dynamic wireless power transfer roadway in-motion electric vehicle charging," in *2023 IEEE Power & Energy Society Innovative Smart Grid Technologies Conference (ISGT)*, 2023, pp. 1–5.

[7] H. Feng, R. Tavakoli, O. C. Onar, and Z. Pantic, "Advances in high-power wireless charging systems: Overview and design considerations," *IEEE Transactions on Transportation Electrification*, vol. 6, no. 3, pp. 886–919, 2020.

[8] L. Tan, W. Zhao, H. Liu, J. Li, and X. Huang, "Design and optimization of ground-side power transmitting coil parameters for EV dynamic wireless charging system," *IEEE Access*, vol. 8, pp. 74 595–74 604, 2020.

[9] D. D. Lewis, H. Gong, G. Erhardt, R. Zeng, O. Onar, V. P. Galigekere, B. Ozpineci, and D. M. Ionel, "Sizing considerations for EV dynamic wireless charging systems with integrated energy storage," in *2022 IEEE Transportation Electrification Conference & Expo (ITEC)*, 2022, pp. 611–616.

[10] T. Newbolt, P. Mandal, H. Wang, and R. Zane, "Priority load control for dynamic WPT roadway in electrified transportation infrastructure," in *2023 IEEE Power and Energy Society General Meeting (PESGM)*, 2023, pp. 1–5.

[11] L. Tan, W. Zhao, M. Ju, H. Liu, and X. Huang, "Research on an EV dynamic wireless charging control method adapting to speed change," *Energies*, vol. 12, no. 11, 2019. [Online]. Available: https://www.mdpi.com/1996-1073/12/11/2214

[12] K. Kumar, K. V. V. S. R. Chowdary, B. Nayak, and V. Mali, "Performance evaluation of dynamic wireless charging system with the speed of electric vehicles," in *2022 IEEE 19th India Council International Conference (INDICON)*, 2022, pp. 1–4.

[13] C. Li, X. Dong, L. M. Cipcigan, M. A. Haddad, M. Sun, J. Liang, and W. Ming, "Economic viability of dynamic wireless charging technology for private EVs," *IEEE Transactions on Transportation Electrification*, vol. 9, no. 1, pp. 1845–1856, 2023.

[14] Y. Wang, R. Yuan, Z. Jiang, S. Zhao, W. Zhao, and X. Huang, "Research on dynamic wireless EV charging power control method based on parameter adjustment according to driving speed," in *2019 IEEE 2nd International Conference on Electronics Technology (ICET)*, 2019, pp. 305–309.

[15] S. Debnath, A. Foote, O. C. Onar, and M. Chinthavali, "Grid impact studies from dynamic wireless charging in smart automated highways," in *2018 IEEE Transportation Electrification Conference and Expo (ITEC)*, 2018, pp. 950–955.

[16] A. O. el Meligy, E. A. Elghanam, M. S. Hassan, and A. H. Osman, "Deployment optimization of dynamic wireless chargers for electric vehicles," in *2021 IEEE Transportation Electrification Conference Expo (ITEC)*, 2021, pp. 113–118.

[17] C. A. García-Vázquez, F. Llorens-Iborra, L. M. Fernández-Ramírez, H. Sánchez-Sainz, and F. Jurado, "Evaluating dynamic wireless charging of electric vehicles moving along a stretch of highway," in *2016 International Symposium on Power Electronics, Electrical Drives, Automation and Motion (SPEEDAM)*, 2016, pp. 61–66.

[18] F. Lu, H. Zhang, H. Hofmann, and C. C. Mi, "A dynamic charging system with reduced output power pulsation for electric vehicles," *IEEE Transactions on Industrial Electronics*, vol. 63, no. 10, pp. 6580–6590, 2016.

[19] A. Zakerian, S. Vaez-Zadeh, and A. Babaki, "A dynamic wpt system with high efficiency and high power factor for electric vehicles," *IEEE Transactions on Power Electronics*, vol. 35, no. 7, pp. 6732–6740, 2020.

[20] C. Wang, C. Zhu, G. Wei, J. Feng, J. Jiang, and R. Lu, "Design of compact three-phase receiver for meander-type dynamic wireless power transfer system," *IEEE Transactions on Power Electronics*, vol. 35, no. 7, pp. 6854–6866, 2020.

[21] H. Wang, U. Pratik, A. Jovicic, N. Hasan, and Z. Pantic, "Dynamic wireless charging of medium power and speed electric vehicles," *IEEE Transactions on Vehicular Technology*, vol. 70, no. 12, pp. 12 552–12 566, 2021.

[22] V. Z. Barsari, D. J. Thrimawithana, and G. A. Covic, "An inductive coupler array for in-motion wireless charging of electric vehicles," *IEEE Transactions on Power Electronics*, vol. 36, no. 9, pp. 9854–9863, 2021.

[23] "Our Wireless Charging Electric Road Projects," Jan. 2022. [Online]. Available: https://electreon.com/projects

[24] "Use Case 3 - Implementing dynamic induction charging infrastructures on long-distance roads," Jul. 2023. [Online]. Available: https://www.incit-ev.eu/use-case-3-implementing-real-life-dynamic-induction-charging-infrastructures-for-long-distance-roads-in-versailles-france/

[25] "ENRX | Wireless charging for dynamic electric roadways." [Online]. Available: https://www.enrx.com/en/Induction-Applications/Inductive-charging-and-power-applications/Dynamic-electric-roadway

[26] D. D. Lewis, O. Onar, V. P. Galigekere, M. Mohammad, and D. M. Ionel, "Optimal power sharing speed compensation in on-road wireless EV charging systems," in *2023 IEEE Transportation Electrification Conference & Expo (ITEC)*, 2023, pp. 1–5.

[27] S. T. Harave, O. Onar, M. Mohammad, V. P. Galigekere, and G.-J. Su, "Efficiency and output power sensitivity to control parameter variations in an LCC-series wireless power transfer system," in *2023 IEEE Transportation Electrification Conference & Expo (ITEC)*, 2023, pp. 1–5.

[28] B. J. Limb, T. H. Bradley, B. Crabb, R. Zane, C. McGinty, and J. C. Quinn, "Economic and environmental feasibility, architecture optimization, and grid impact of dynamic charging of electric vehicles using wireless power transfer," in *6th Hybrid and Electric Vehicles Conference (HEVC 2016)*, 2016, pp. 1–6.

[29] D. Haddad, T. Konstantinou, A. Prasad, Z. Hua, D. Aliprantis, K. Gkritza, and S. Pekarek, "Data-driven design and assessment of dynamic wireless charging systems," in *2019 IEEE PELS Workshop on Emerging Technologies: Wireless Power Transfer (WoW)*, 2019, pp. 59–64.

[30] R. Zeng, V. P. Galigekere, O. C. Onar, and B. Ozpineci, "Grid integration and impact analysis of high-power dynamic wireless charging system in distribution network," *IEEE Access*, vol. 9, pp. 6746–6755, 2021.

[31] O. Hafez and K. Bhattacharya, "Integrating EV charging stations as smart loads for demand response provisions in distribution systems," *IEEE Transactions on Smart Grid*, vol. 9, no. 2, pp. 1096–1106, Mar. 2018.

[32] T. Theodoropoulos, A. Amditis, J. Sallan, H. Bludszuweit, B. Berseneff, P. Guglielmi, and F. Deflorio, "Impact of dynamic EV wireless charging on the grid," in *2014 IEEE International Electric Vehicle Conference (IEVC)*. Florence: IEEE, Dec. 2014, pp. 1–7.

[33] T. Newbolt, P. Mandal, H. Wang, and R. Zane, "Sustainability of dynamic wireless power transfer roadway for in-motion electric vehicle charging," *IEEE Transactions on Transportation Electrification*, vol. 10, no. 1, pp. 1347–1362, 2024.

[34] "Traffic Counts," publisher: Kentucky Transportation Cabinet. [Online]. Available: https://maps.kytc.ky.gov/trafficcounts/

[35] O. C. Onar, M. Chinthavali, S. L. Campbell, L. E. Seiber, and C. P. White, "Vehicular integration of wireless power transfer systems and hardware interoperability case studies," *IEEE Transactions on Industry Applications*, vol. 55, no. 5, pp. 5223–5234, 2019.

[36] M. Mohammad, O. C. Onar, G.-J. Su, J. Pries, V. P. Galigekere, S. Anwar, E. Asa, J. Wilkins, R. Wiles, C. P. White, and L. E. Seiber, "Bidirectional LCC–LCC-compensated 20-kW wireless power transfer system for medium-duty vehicle charging," *IEEE Transactions on Transportation Electrification*, vol. 7, no. 3, pp. 1205–1218, 2021.

[37] D. Purushothaman, R. Narayanamoorthi, A. Elrashidi, and H. Kotb, "A comprehensive review on single-stage wpt converter topologies and power factor correction methodologies in EV charging," *IEEE Access*, vol. 11, pp. 135 529–135 555, 2023.

[38] C.-H. Jo and D.-H. Kim, "Novel compensation parameter design methodology and maximum efficiency tracking control strategy for inductive power transfer system," *IEEE Access*, vol. 10, pp. 56 133–56 144, 2022.

[39] L. Xue, V. Galigekere, E. Gurpinar, G.-j. Su, S. Chowdhury, M. Mohammad, and O. Onar, "Modular power electronics approach for high power dynamic wireless charging system," *IEEE Transactions on Transportation Electrification*, pp. 1–1, 2023.

[40] V. P. Galigekere, O. Onar, J. Pries, S. Zou, Z. Wang, and M. Chinthavali, "Sensitivity analysis of primary-side LCC and secondary-side series compensated wireless charging system," in *2018 IEEE Transportation Electrification Conference and Expo (ITEC)*, 2018, pp. 885–891.

[41] U. D. Kavimandan, V. P. Galigekere, O. Onar, M. Mohammad, B. Ozpineci, and S. M. Mahajan, "The sensitivity analysis of coil misalignment for a 200-kW dynamic wireless power transfer system with an LCC-S and LCC-P compensation," in *2021 IEEE Transportation Electrification Conference & Expo (ITEC)*, 2021, pp. 1–8.

[42] M. Budhia, J. T. Boys, G. A. Covic, and C.-Y. Huang, "Development of a single-sided flux magnetic coupler for electric vehicle IPT charging systems," *IEEE Transactions on Industrial Electronics*, vol. 60, no. 1, pp. 318–328, 2013.

[43] A. Zaheer, M. Neath, H. Z. Z. Beh, and G. A. Covic, "A dynamic EV charging system for slow moving traffic applications," *IEEE Transactions on Transportation Electrification*, vol. 3, no. 2, pp. 354–369, 2017.

[44] I. Karakitsios, F. Palaiogiannis, A. Markou, and N. D. Hatziargyriou, "Optimizing the energy transfer, with a high system efficiency in dynamic inductive charging of EVs," *IEEE Transactions on Vehicular Technology*, vol. 67, no. 6, pp. 4728–4742, 2018.

[45] D.-H. Kim, S. Kim, S.-W. Kim, J. Moon, I. Cho, and D. Ahn, "Coupling extraction and maximum efficiency tracking for multiple concurrent transmitters in dynamic wireless charging," *IEEE Transactions on Power Electronics*, vol. 35, no. 8, pp. 7853–7862, 2020.

[46] V. Galigekere and B. Ozpineci, "High Power and Dynamic Wireless Charging of Electric Vehicles (EVs)." [Online]. Available: https://www.energy.gov/eere/vehicles/articles/high-power-and-dynamic-wireless-charging-electric-vehicles-evs

[47] O. C. Onar, "High Power and Dynamic Wireless Charging of Electric Vehicles (EVs)," Buenos Aires, Argentina, Sep. 2022. [Online]. Available: https://www.piarc.org/en/activities/PIARC-International-Seminars-Proceedings/International-Seminars-2022-PIARC-World-Road-Association/International-Seminar-Building-Smart-Approaches-Freight-Road-Network-Operations-ITS-Technology-Buenos-Aires-Argentina-September-2022

[48] O. Onar, V. P. Galigekere, J. Pries, G.-J. Su, S. Zou, S. Anwar, J. Wilkins, R. Wiles, L. Seiber, and C. White, "Modeling, design, and experimental verification of a WPT level-3 wireless charger with compact secondary coupler," in *2019 IEEE Applied Power Electronics Conference and Exposition (APEC)*, 2019, pp. 1722–1729.